DESIGN OF SLENDER BRICK ELEMENTS BASED ON STABILITY CRITERIA

by

M. A. Hatzinikolas[1], J. Longworth[2], and J. Warwaruk[3]

1 Director of Technical Services, Alberta Masonry Institute, Edmonton, Alberta, Canada.

2 Professor of Civil Engineering Dept., University of Alberta, Edmonton, Alberta, Canada.

3 Professor of Civil Engineering Dept., University of Alberta, Edmonton, Alberta, Canada.

ALBERTA MASONRY INSTITUTE

DESIGN OF SLENDER BRICK ELEMENTS BASED ON STABILITY CRITERIA

by

M.A. Hatzinikolas[1], J. Longworth[2] and J. Warwaruk[3]

Abstract

In the design of load bearing masonry structures, subjected to the combined action of vertical and lateral loads, it is necessary to account for the effect of lateral deflections, or the so-called P-Δ effect. In North America the moment magnifier method has been extensively applied in the evaluation of the P-Δ effect in steel and reinforced concrete beam columns. This method can also be satisfactorily applied in the case of masonry structures.

This paper presents the application of the moment magnifier method to the analysis of load bearing brick walls. The analytical results are compared with results of tests of large brick wall panels.

---

[1] Director of Technical Services, Alberta Masonry Institute, Edmonton, Alberta, Canada.

[2] Professor of Civil Engineering Dept., University of Alberta, Edmonton, Alberta, Canada.

[3] Professor of Civil Engineering Dept., University of Alberta, Edmonton, Alberta, Canada.

Introduction

The complete, accurate analysis of a structural member subjected to axial compression and bending must include the effect of lateral deflections on moments throughout the length of the member. This effect is commonly referred to as the P-Δ effect. Various methods for such analysis have been summarized by MacGregor (1). The P-Δ effect magnifies the primary moments; thus the reason for describing one method of analysis as the moment magnifier method.

Canadian design standards for structural steel and reinforced concrete (2), (3) employ the concept of moment magnification in the design procedures for members subjected to axial load and bending. The moment magnifier method has been shown by the authors (4) to satisfactorily predict the behavior of concrete masonry walls. In the present study the moment magnifier method is applied to brick walls and the analytical results are compared with the results of an experimental investigation.

Analysis

To account for the effect of lateral deflections in a vertical structural member subjected to eccentric compression forces applied with equal eccentricities at the member ends, the moment magnifier analysis gives the value

of the resulting maximum moment as

$$M = \frac{Pe}{(1 - P/P_{cr})} \qquad (1)$$

where P = applied vertical load

e = eccentricity of vertical load

P_{cr} = critical buckling load

If the end eccentricities are not equal, the resulting maximum moment may be expressed as

$$M = Pe \frac{C_m}{(1 - P/P_{cr})} \qquad (2)$$

where C_m = a factor which converts the given end moment condition to an equivalent equal end moment condition.

For end eccentricities e_1 and e_2 where $e_1 < e_2$

$$C_m = 0.6 + 0.4 \frac{e_1}{e_2} \qquad (3)$$

An acceptable value for the critical buckling load is

$$P_{cr} = 8\pi^2 (0.5 - e/t)^3 \frac{EI_o}{h^2} \qquad (4)$$

where t = wall thickness

I_o = moment of inertia of gross cross section or $\frac{bt^3}{12}$ where b = wall width

h = wall height

E = modulus of elasticity

Letting $I_1 = 8(0.5 - e/t)^3 I_o$

$$P_{cr} = \pi^2 \frac{EI_1}{h^2} \tag{5}$$

If we consider that masonry possesses some tensile strength f_t', the conditions on the cross section will correspond to Figure 1. Cracks penetrate to the point where the tension stress equals f_t' and

$$I_1 = 8(0.5 - e/t + \frac{\zeta}{2t})^3 I_o \tag{6}$$

where ζ is the distance from the point of zero stress to the end of the crack. This distance is obtained from the following equations.

$$f_{max} = \frac{4}{3} \{\frac{P}{A(1 - 2\frac{e}{t})}\} \tag{7}$$

$$\xi = \frac{2tP}{Af_{max}} \tag{8}$$

$$\zeta = \frac{\xi f_t'}{f_{max}} \tag{9}$$

If the wall is subjected to unequal end eccentricities, e_1 and e_2, producing single curvature bending, the value of e in Equation (7) may be taken as equal to the average of e_1 and e_2. Although this is an approximation, it gives satisfactory results.

A method for determining the buckling load for a wall in double curvature bending is presented in Reference (5).

Although walls bent in double curvature may be expected to crack as shown in Figure 2, the buckling configuration tends to be the primary single loop configuration shown in Figure 3. This behaviour is verified by typical test results shown in Figure 9. As a result, it is possible to represent the wall as an equivalent "stepped" wall shown in Figure 4. The critical buckling load for such a structure may be expressed as

$$P_{cr} = \lambda \frac{EI_o}{h^2} \qquad (10)$$

where λ is a buckling coefficient for the "stepped" wall which depends on $\alpha = e_1/(e_1 + e_2)$ and $\beta = I_1/I_o$. Values of λ are tabulated in Table 1 and a more extensive tabulation is included in Reference (5).

The mode of failure of masonry walls is affected by the magnitude of the end eccentricities. It has been shown by the authors (6) that for initial end eccentricities greater than t/20, concrete block masonry fails when the compressive strength of the units is reached. For eccentricities smaller than t/20, failure occurs by vertical splitting of the units.

An interaction diagram provides an effective means of describing the behavior of an eccentrically loaded masonry wall. Such a diagram is a graph of vertical load vs maximum moment, and is dependent on height and thickness of the wall, end eccentricities and material properties.

A primary interaction diagram may be constructed on the basis of strength, i.e. considering h/t = 0, for which case there are no slenderness effects. Based on wall dimensions, eccentricity and material properties it can be shown (7) that the interaction diagram is defined by the following two equations:

$$M = (P_o - P)\frac{t}{6} \quad \text{for} \quad \frac{P}{P_o} \geq 0.5 \tag{11}$$

and

$$M = \left(1 - \frac{4}{3}\frac{P}{P_o}\right)\frac{Pt}{2} \quad \text{for} \quad \frac{P}{P_o} \leq 0.5 \tag{12}$$

where M = resisting moment

P = vertical load

P_o = compressive strength, f'_m, times net mortar bedded area, A_m

Figures 11 and 12 show interaction diagrams based on these equations for the case of $f'_m = 18.6 N/mm^2$, $A_m = 69930\ mm^2$ and $t = 190$ mm, values which correspond to the properties of specimens tested in the experimental portion of the present study.

To establish an interaction diagram for $\frac{h}{t} > 0$, slenderness effects must be taken into account. With increased slenderness, lateral deflection increases in eccentrically loaded walls. This fact is reflected in the value of the critical buckling load P_{cr} which is a factor in the equation for magnified moment. An iterative procedure

must be employed in order to establish points on the interaction diagram. The procedure for determining the point on the diagram for a particular e/t value consists of the following steps:

1. For the particular e/t ratio, obtain values of P and M from the interaction diagram based on h/t = 0.
2. Calculate P_{cr}.
3. Calculate a revised value for P.
4. Repeat steps 1 to 3 until convergence occurs.

Convergence is rapid and only two or three cycles are normally necessary to obtain the correct values of P and M for the interaction diagram.

The following example illustrates typical calculations in the iterative procedure.

Given: $b = 1000$ mm

$t = 190$ mm

$h = 3900$ mm

$e_1 = e_2 = t/3$ (single curvature bending)

$f'_t = 1.38$ N/mm^2

$E = 13.44 \times 10^3$ N/mm^2

$I_o = \frac{bt^3}{11} = 5.72 \times 10^8$ mm^4

From Figure 11, for $\frac{h}{t} = 0$,

$P = 325$ kN

Then $M = Pe = 20.5$ kNm

From Equation (7) $f_{max} = 3.31$ N/mm^2

From Equation (8) $\xi = 190$ mm

From Equation (9) $\zeta = 80$ mm

From Equation (6) $I_1 = 0.432\ I_o$

From Equation (5) $P_{cr} = 2020$ kN

Substituting in Equation (1)

$$20.5 = \frac{P \times 63.3 \times 10^{-3}}{1 - \frac{P}{2020}}$$

from which $P = 280$ kN

This is the end of the first cycle of iteration. The second cycle begins with P = 280 kN and M = Pe = 17.7 kNm. After the second cycle P converges to a value of 260 kN.

The complete interaction diagram for h/t = 20.5 is shown in Figure 11.

Experimental Program

Materials

Two core 190 x 90 x 390 mm pressed clay units, as shown in Figure 5, were used in the test specimens. Based on tests on six 33 x 58 x 92 mm solid specimens cut from the units, the average compressive strength of the material was 21.2 N/mm^2. The h/t ratio of these specimens was 2.79. The average compressive strength of six whole units was 18.6 N/mm^2.

Mortar used in building the test specimens was factory produced (ready mixed) mortar delivered to the laboratory by the supplier. The composition of the mortar conformed to the requirements of type N mortar as defined by CSA Standard A179-1975 (8). The average compressive strength at 28 days was 7.4 N/mm^2.

The compressive strength of the masonry assembly was determined from tests on 5 short specimens shown in Figure 6. The slenderness ratio of these specimens was 3.14. The average compressive strength based on gross cross-sectional area was 5.3 N/mm^2, and the compressive strength based on net mortar bedded area was 14.5 N/mm^2.

Wall Specimens

Ten plain wall specimens were tested. All specimens were 190 x 1000 x 3600 mm. They were constructed by an experienced mason and allowed to cure in laboratory environment for a minimum of 28 days. No horizontal or vertical reinforcement was used. To avoid local failures during testing, the top and bottom courses in all walls were fully grouted with fine grout.

Test Procedure

The wall specimens were tested to failure in a 6225 kN capacity hydraulic testing machine. End eccentricities were varied to include conditions of axial load, single curvature bending and double curvature bending as

indicated in Table 2. Figure 7 shows a typical specimen in the testing machine. Lateral deflections at five equally spaced elevations were measured by means of LVDT units at various loads prior to failure.

Test Results

The results of the tests of the 10 wall specimens are summarized in Table 2. Typical deflected shapes are presented in Figures 8 and 9. Test results are plotted in Figures 11 and 12 for comparison with theoretical interaction diagrams.

All walls tested in double curvature bending deflected in a single loop configuration as shown in Figure 9. As shown in Table 2, walls tested in single curvature bending deflected appreciably more than walls tested in double curvature bending. In general there was good agreement between analytical and test values of failure loads.

Conclusion

Results of this study indicate that the moment magnifier method satisfactorily accounts for slenderness effects, i.e. the P-Δ effect, in eccentrically loaded brick masonry walls. This is confirmed from results of ten tests covering a range of end eccentricities, including single curvature bending and double curvature bending.

Acknowledgements

The research program on which this paper is based was conducted at the University of Alberta and was made possible by research funds provided by the National Sciences and Engineering Research Council of Canada and the Alberta Masonry Institute. Giant brick units were donated by IXL Industries Ltd., and ready mixed mortar was donated by North American Mortar Supply Co.

References

1. MacGregor, J.G., "Stability of Reinforced Concrete Building Frames", State of the Art paper No. 1, Technical Committee 23, Proceedings of the International Conference on Planning and Design of Tall Buildings, Volume 3, American Society of Civil Engineers, New York, 1973, pp. 19-35.

2. CSA Standard A23.3-M77, Code for the Design of Concrete Structures for Buildings, Canadian Standards Association, Rexdale, Ontario, Canada, 1977.

3. CSA Standard S16.1-M78, Steel Structures for Buildings - Limit States Design, Canadian Standards Association, Rexdale, Ontario, Canada, 1978.

4. Hatzinikolas, M., Longworth, J. and Warwaruk, J., "The Analysis of Eccentrically Loaded Masonry Walls by the Moment Magnifier Method", Proceedings of the Second Canadian Masonry Symposium, Ottawa, Canada, 1980, pp. 245-258.

5. Hatzinikolas, M., Longworth, J. and Warwaruk, J., "Buckling of Plain Masonry Walls with Initial Double Curvature", Proceedings of the North American Masonry Conference, University of Colorado, Boulder, Colorado, August, 1978. pp. 87-1 to 87-14.

6. Hatzinikolas, M., Longworth, J. and Warwaruk, J. "Failure Modes for Concrete Block Walls", Journal of the American Concrete Institute, Proceedings V.77, No. 4, July-August, 1980, pp. 258-263.

7. Yokel, F.Y., Mathey, R.G. and Dikkers, R.D., "Strength of Masonry Walls Under Compressive and Transverse Loads", Building Science Series 34, National Bureau of Standards, Washington, U.S.A.

8. CSA Standard A179-1975 Mortar and Grout for Unit Masonry, Canadian Standards Association, Rexdale, Ontario, Canada, 1975.

TABLE 1 Buckling Coefficients for Stepped Walls and Columns

β \ α	0.0	0.10	0.20	0.30	0.40	0.50	0.60	0.70	0.80	0.90	1.00
0.10	0.99	1.02	1.11	1.26	1.58	2.35	3.67	5.47	7.99	9.74	9.88
0.20	1.98	2.01	2.18	2.39	2.79	3.66	5.17	7.08	8.85	9.78	9.88
0.30	2.98	2.99	3.18	3.45	3.92	4.78	6.20	7.88	9.18	9.80	9.88
0.40	3.95	3.98	4.15	4.47	4.95	5.77	7.02	8.39	9.36	9.82	9.88
0.50	4.94	4.96	5.12	5.44	5.92	6.66	7.69	8.76	9.51	9.88	9.88
0.60	5.93	5.95	6.09	6.38	6.82	7.44	8.26	9.06	9.61	9.84	9.88
0.70	6.91	6.93	7.04	7.29	7.65	8.15	8.75	9.31	9.89	9.85	9.88
0.80	7.90	7.91	7.99	8.17	8.44	8.79	9.17	9.53	9.78	9.86	9.88
0.90	8.89	8.89	8.94	9.03	9.16	9.36	9.55	9.71	9.82	9.87	9.88
1.00	9.88	9.88	9.88	9.88	9.88	9.88	9.88	9.88	9.88	9.88	9.88

Note: $\alpha = \dfrac{e_1}{e_1 + e_2}$

$\beta = \dfrac{I_1}{I_o}$

TABLE 2 Summary of Test Results

Wall	Eccentricity e_1	Eccentricity e_2	Vertical Load kN	Maximum Deflection mm	Maximum Moment kNm	Type of Failure
1	0	0	850	10	8.5	splitting, crushing
2	0	0	775	3	2.0	splitting
3	t/12	t/12	791	11	21.2	
4	t/12	t/12	645	14	19.2	crushing
5	t/12	t/12	649	17	21.8	
6	t/6	t/6	602	21	31.5	crushing
7	t/3	t/3	203	10	14.9	crushing
8	t/12	-t/12	725	3	11.4	crushing
9	t/6	-t/6	638	2	20.2	crushing
10	t/3	-t/3	429	3	27.1	crushing

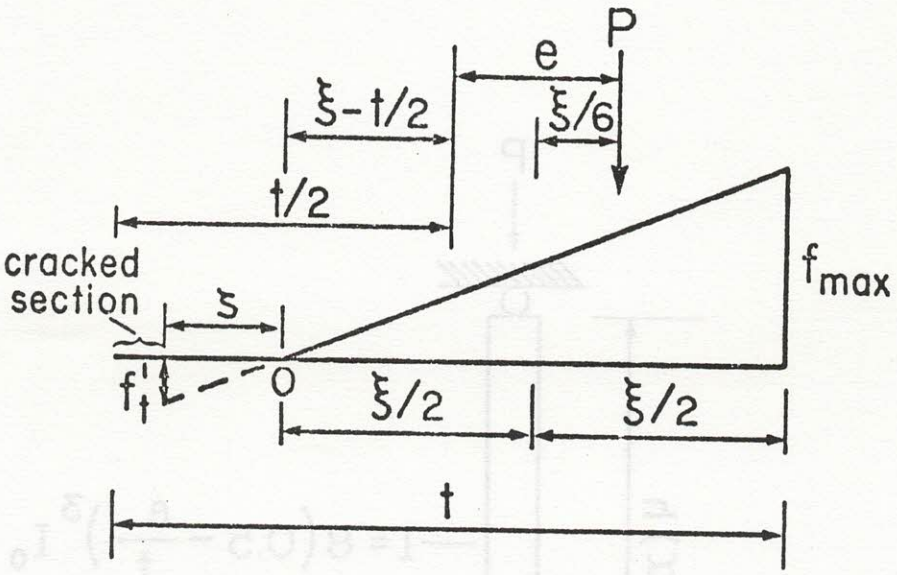

Figure 1 Stress Distribution on Masonry Section

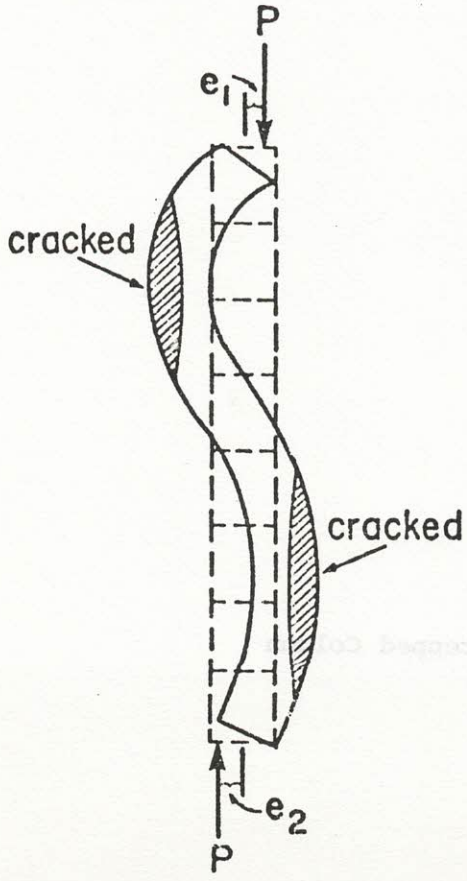

Figure 2 Wall Bent in Double Curvature

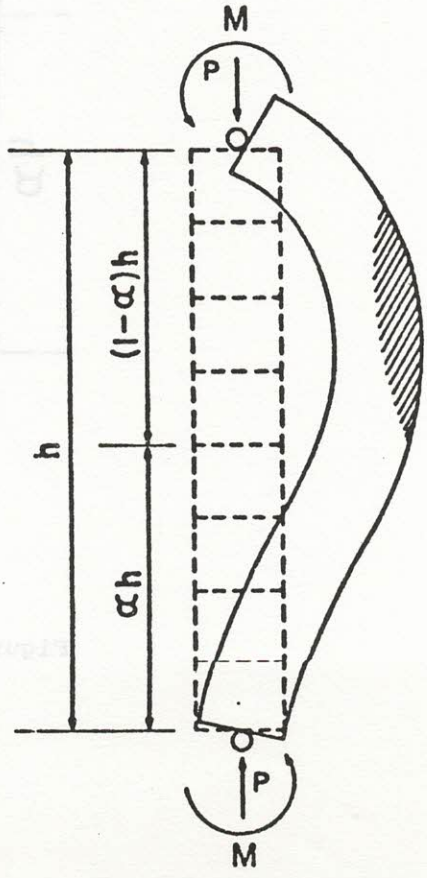

Figure 3 Buckling Mode for Wall in Double Curvature

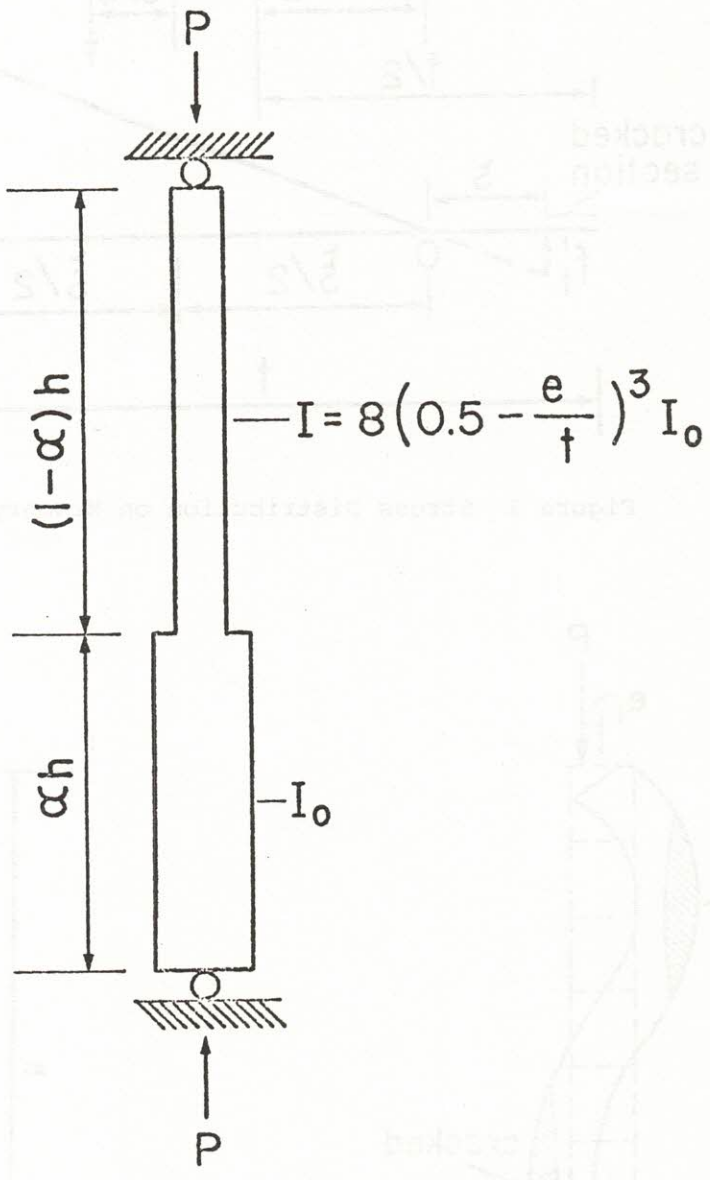

Figure 4 Equivalent Stepped Column

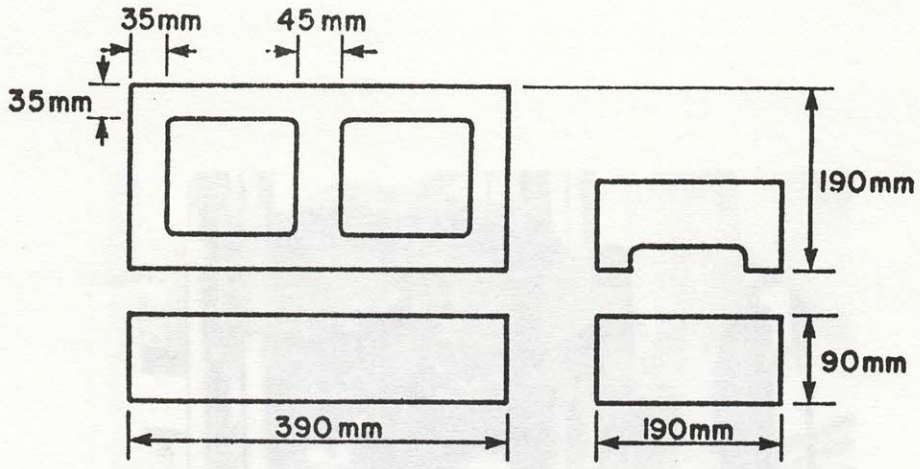

Figure 5 Giant Brick Unit

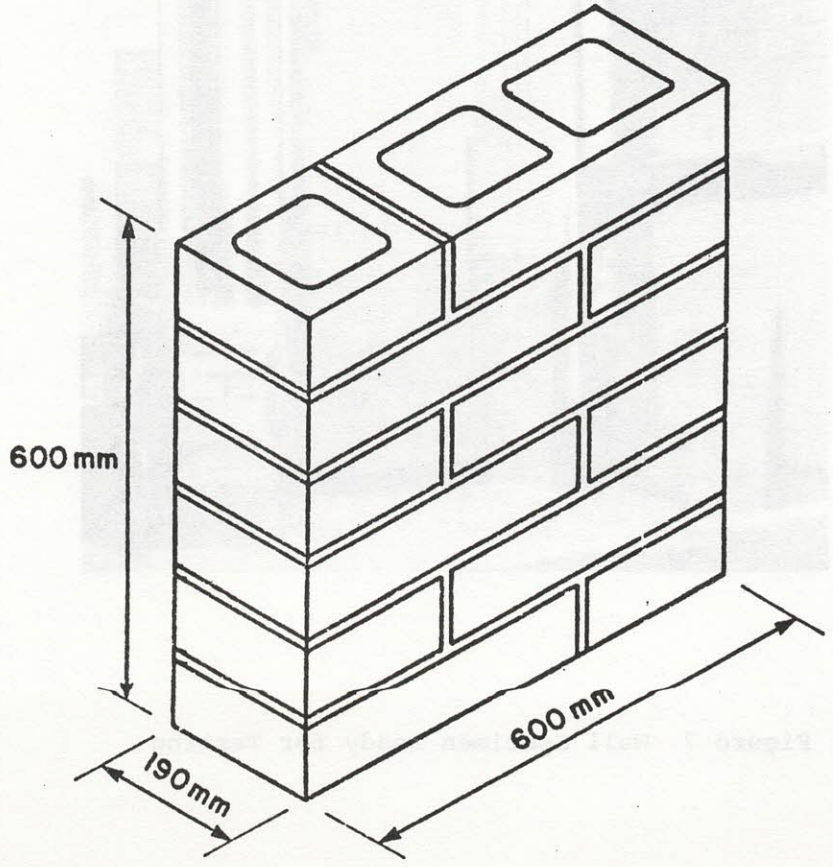

Figure 6 Short Wall Specimen

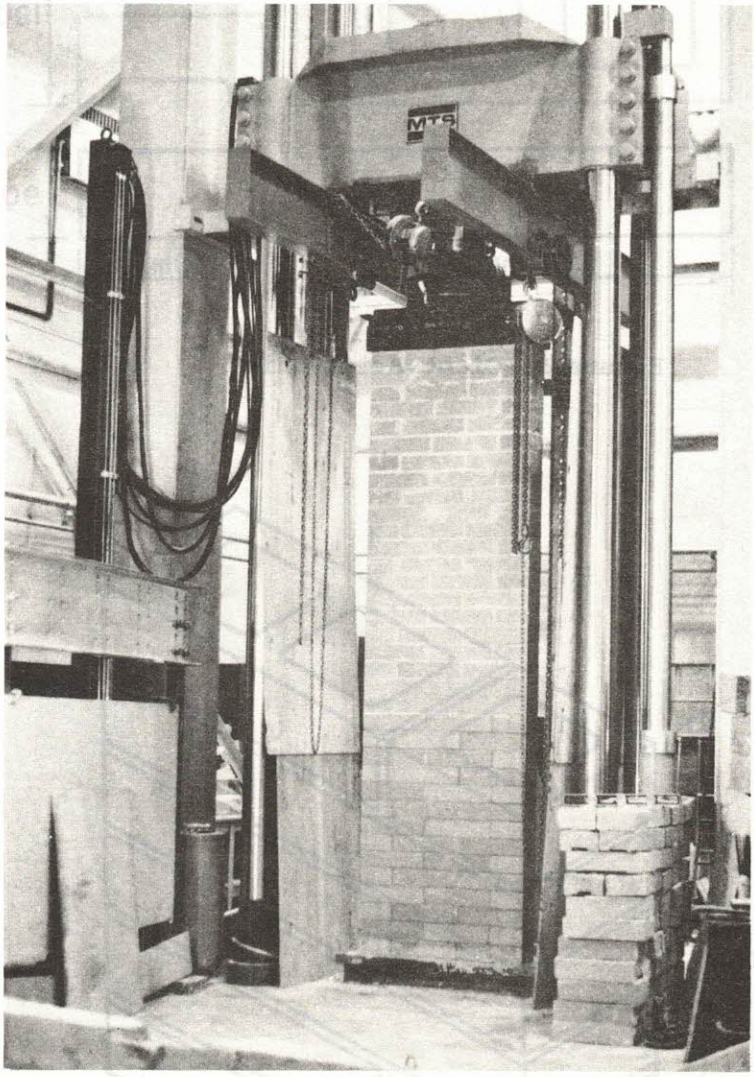

Figure 7 Wall Specimen Ready for Testing

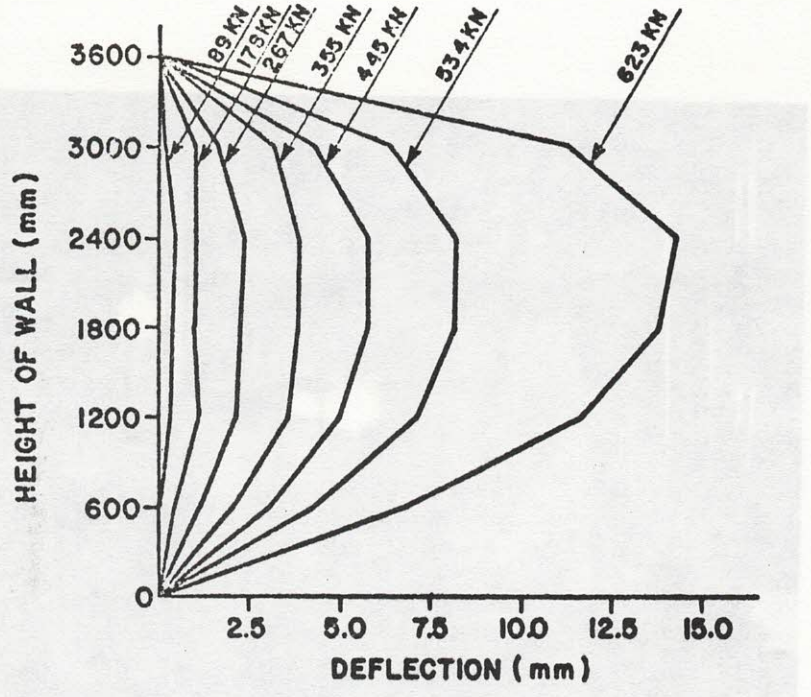

Figure 8 Deflected Shape of Wall in Single Curvature

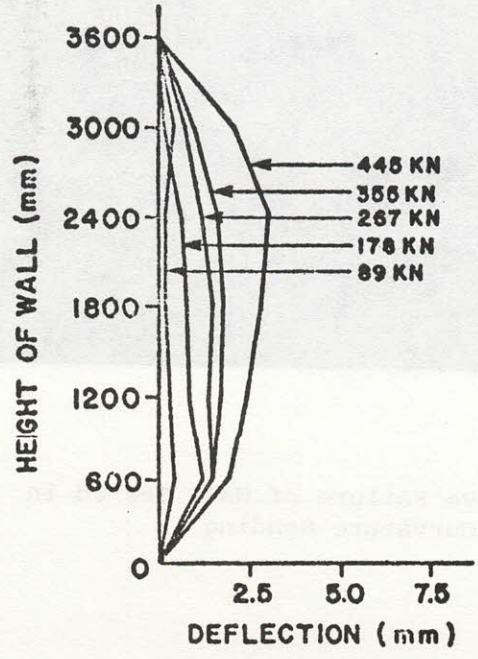

Figure 9 Deflected Shape of Wall in Double Curvature

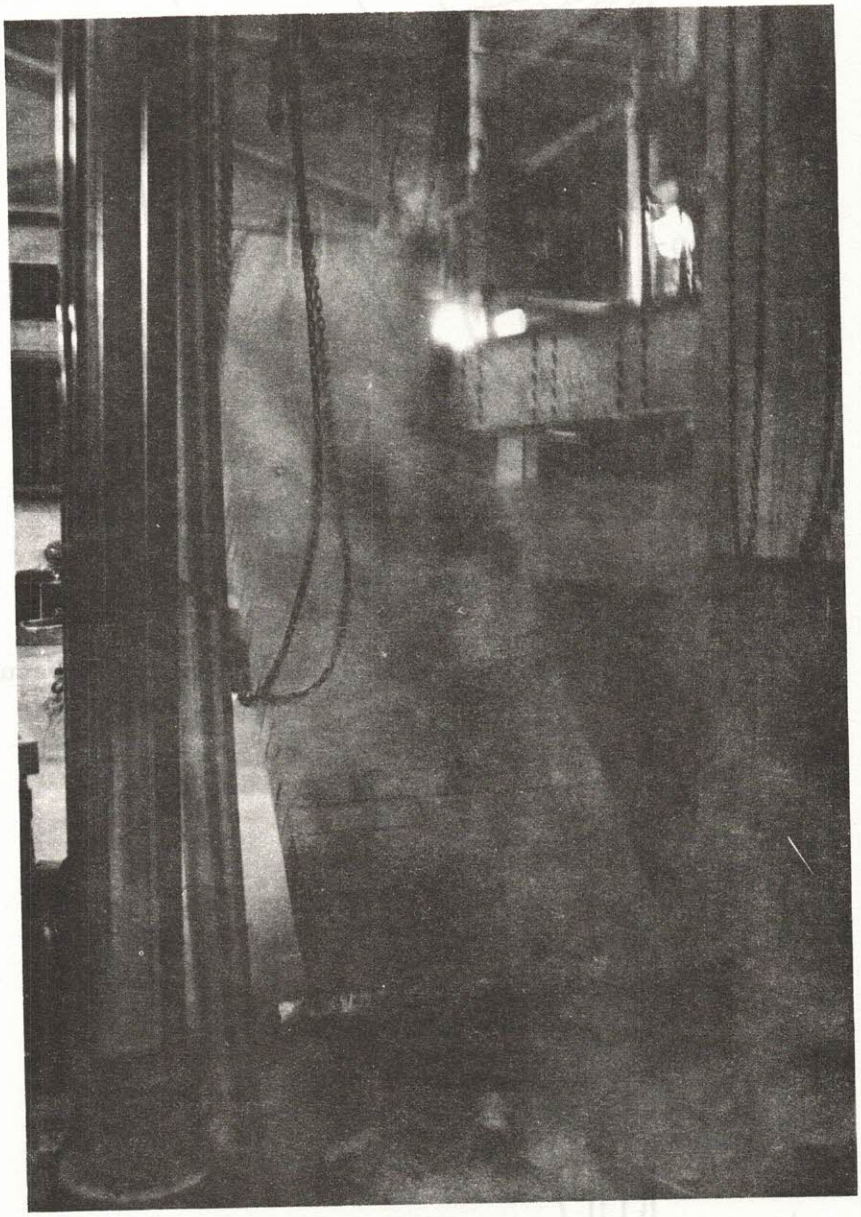

Figure 10 Explosive Failure of Wall Tested in Double Curvature Bending

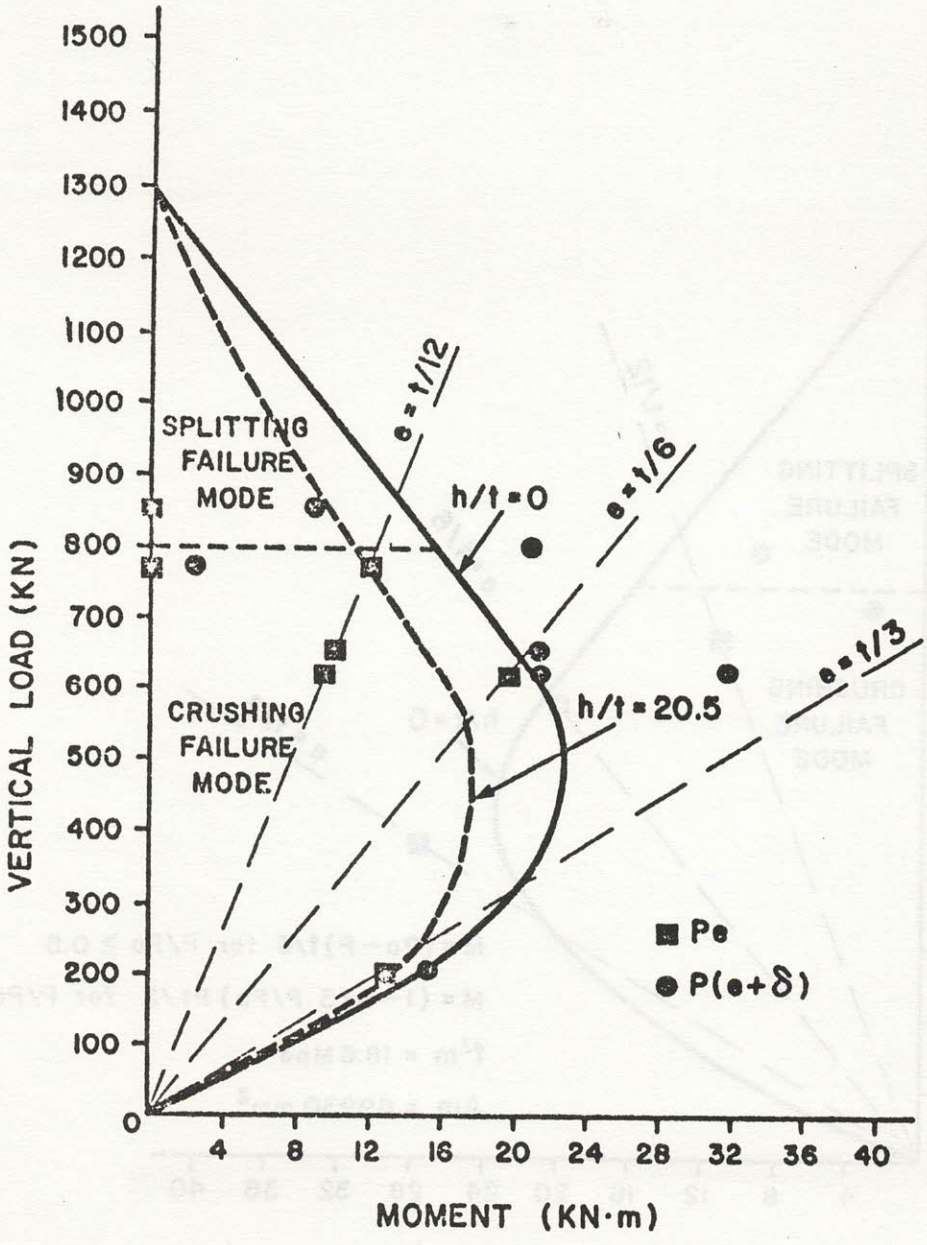

Figure 11 Interaction Diagram for Walls in Single Curvature Bending

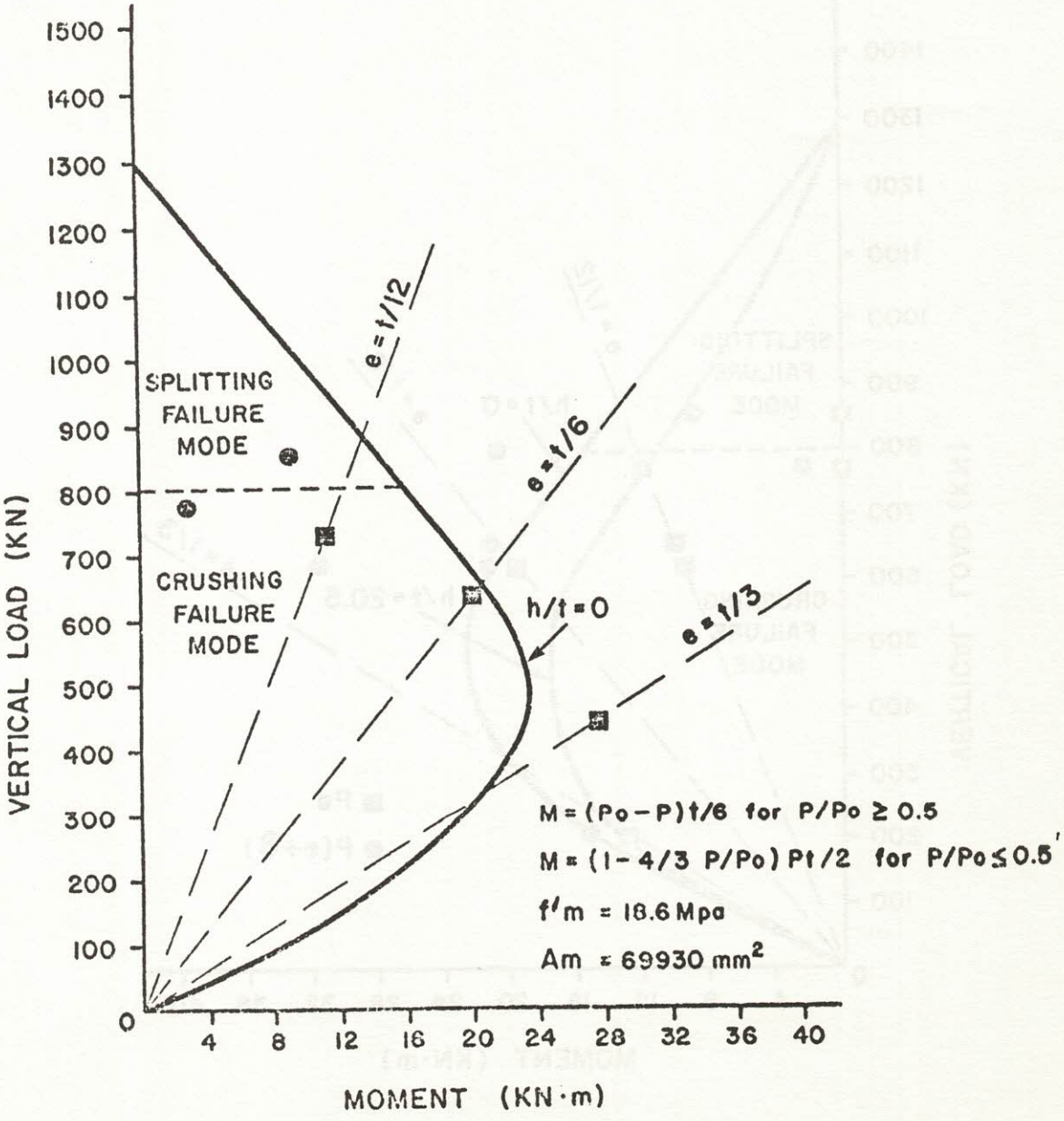

Figure 12 Interaction Diagram for Walls in Double Curvature Bending